

Galerkin Solution of Stochastic Beam Bending on Winkler Foundations

C. R. A. Silva¹, H. P. Azikri de Deus¹, G.E. Mantovani² and A.T. Beck³

Abstract: In this paper, the Askey-Wiener scheme and the Galerkin method are used to obtain approximate solutions to stochastic beam bending on Winkler foundation. The study addresses Euler-Bernoulli beams with uncertainty in the bending stiffness modulus and in the stiffness of the foundation. Uncertainties are represented by parameterized stochastic processes. The random behavior of beam response is modeled using the Askey-Wiener scheme. One contribution of the paper is a sketch of proof of existence and uniqueness of the solution to problems involving fourth order operators applied to random fields. From the approximate Galerkin solution, expected value and variance of beam displacement responses are derived, and compared with corresponding estimates obtained via Monte Carlo simulation. Results show very fast convergence and excellent accuracies in comparison to Monte Carlo simulation. The Askey-Wiener Galerkin scheme presented herein is shown to be a theoretically solid and numerically efficient method for the solution of stochastic problems in engineering.

Keywords: Euler-Bernoulli beam, Galerkin method, Winkler foundation, Askey-Wiener scheme, tensor product, stochastic processes, Monte Carlo simulation.

1 Introduction

The field of stochastic mechanics has been subject of extensive research and significant developments in recent years. Stochastic mechanics incorporates the modeling of randomness or uncertainty in the mathematical formulation of mechanics problems. This is in contrast to the more established field of structural reliability, where uncertainty and randomness are also addressed, but where problem solutions are obtained mainly based on deterministic mechanics models.

¹ Academic Department of Mechanics, Federal Technological University of Paraná / PPGEM-UTFPR / PPGMNE-UFPR, Curitiba, PR, Brazil.

² Federal Technological University of Parana, Curitiba, Brazil.

³ Department of Structural Engineering, University of Sao Paulo, Sao Carlos, SP, Brazil.

The analysis of stochastic engineering systems has received new impulse with use of finite element methods to obtain response statistics. Initially, finite element solutions were combined with the Monte Carlo method, and statistics were obtained from realizations of system response. This system sampling technique was employed by Yamazaki, Shinozuka and Dasgupta (1988), who used the Neumann series to obtain realizations of the system. Hisada and Nakagiri (1981) introduced the perturbation technique to obtain the statistics of system response. Araújo and Awruch (1994) used the same technique to obtain response statistics for non-linear structures subject to static and dynamic loading.

At the end of the 80's, Spanos and Ghanem (1989) used the Galerkin finite element method to solve a stochastic beam bending problem, where Young's modulus was modeled as a Gaussian stochastic process. The space of approximate solutions was built using the finite element method and chaos polynomials. These polynomials form a complete orthonormal system in $L^2(\Omega, \mathcal{F}, P) = \overline{\Psi}^{L^2(\Omega, \mathcal{F}, P)}$, where $\Psi = \text{span}[\{\psi_i\}_{i=0}^{\infty}]$ is the space generated by the chaos polynomials, and (Ω, \mathcal{F}, P) is a probability space. The ideas presented in this study were innovative and represented a new method to solve stochastic problems.

Babuska, Tempone and Zouraris (2005) presented a stochastic version of the Lax-Milgram lemma. The paper presents a hypothesis which represents limitations to the modeling of uncertainty via Gaussian processes. For certain problems of mechanics, use of Gaussian processes can lead to loss of coercivity of the bi-linear form associated to the stochastic problem. This difficulty was encountered in a study by the author (Silva Jr., 2004) and resulted in non-convergence of the solution for the bending of Kirchhoff plates with random parameters. This lack of convergence was due to the choice of a Gaussian process to represent the uncertainty in some (strictly positive) parameters of the system. This failure to converge also affects solutions based on perturbation or simulation methods. Despite this fact, it is easy to find scientific papers published in the 90's that used stochastic Gaussian processes to model intrinsically limited or strictly positive properties. In this line, it is possible to quote: Liu and Liu (1996) studied the spectral response of concrete structures with uncertainty in material properties and in ambient temperature; Anders and Hori (1999) applied the method in non-linear problems involving bodies with elastoplastic behavior and uncertain strength-related mechanical properties. Elman and Furnival (2007) applied a multiscale strategy to obtain numerical solutions to the steady state diffusion problem with uncertainty in the diffusion coefficient. In this last reference, the Karhunen-Loève expansion is used to model stochastic diffusion as a Gaussian process. The authors recognize the technical inconsistency of their approach, but they justify it by some heuristics and by limiting their examples to small variances of the diffusion coefficient. Such reasoning is not

sufficient to ensure existence and uniqueness of solutions, following the theoretical results by Babuska and Chatzipantelidis (2002). It is important to mention that with a suitable choice of parameters it is acceptable to use a beta distribution instead of a Gaussian distribution with small variance. Such an approach would satisfy the technical issues of existence, uniqueness and of uncertain representation.

Considering what has been exposed, the present paper introduces an original application of the Lax-Milgram lemma to justify the existence and uniqueness of the solution of an Euler-Bernoulli beam bending problem. The beam is supported on a Winkler foundation, and uncertainty is considered in beam and foundation stiffness parameters.

The Askey-Wiener scheme was presented by Xiu et al. (2002). This scheme represents a family of polynomials which generate dense probability spaces with probability measures defined on limited support. This enhances the possibilities for uncertain system parameter modeling. In recent years, much effort is being addressed at representing uncertainty in stochastic engineering systems via non-Gaussian processes.

The stochastic beam bending problem has been studied by several authors. Baker and Zeitoun (1990) employed the Adomian method to evaluate convergence properties and estimates of the first and second order moments of the stochastic displacement process for an infinite beam on Winkler foundation. Vanmarcke and Grigoriu (1983) studied the bending of Timoshenko beams with random shear modulus. Elishakoff, Ren and Shinozuka (1995) employed the theory of mean square calculus to construct a solution to the boundary value problem of beam bending with stochastic bending modulus. Ghanem and Spanos (1991) used the Galerkin method and the Karhunen-Loeve series to represent uncertainty in the bending modulus by means of a Gaussian process. Chakraborty and Sarkar (2000) used the Neumann series and Monte Carlo simulation to obtain statistical moments of the displacements of curved beams on Winkler foundation, with uncertainty in the elasticity modulus of the foundation. Singh and Kumar (2008) used finite element and perturbation methods to obtain the statistics of the transverse displacement of a composite plate on a non-linear Winkler/Pasternak foundation. The papers cited above presented numerical solutions to the stochastic beam bending problem, but none addressed the issue of existence and uniqueness of the solutions.

In this paper, the Galerkin method is used to obtain approximate solutions for the bending of Euler-Bernoulli beams on Winkler foundation, with uncertain beam and foundation stiffness. This uncertainty is represented by means of parameterized stochastic processes (Grigoriu, 1995). The approximated solution space is constructed using isomorphism properties between Sobolev and product spaces, using density between continuous functions and Sobolev spaces and using spaces gener-

ated by $L^2(\Omega, \mathcal{F}, P)$ polynomials of the Askey-Wiener scheme (Xiu et al., 2002). An additional contribution of this paper is use of the Lax-Milgram lemma, for a brief study about existence and uniqueness of the solution to stochastic beam bending on Winkler foundation. Two numerical stochastic beam bending examples are also presented. To evaluate the performance of the developed technique, expected value and variance of the transverse displacement processes are determined, and compared with the corresponding estimates obtained via Monte Carlo Simulation.

2 Problem Definition

Let (Ω, \mathcal{F}, P) be a probability space, where Ω is a sample space, \mathcal{F} is an σ -algebra and P is a probability measure. The stochastic beam bending on Winkler foundation problem is defined as:

$$\begin{cases} \frac{d^2}{dx^2} \left(EI \cdot \frac{d^2 u}{dx^2} \right) + \kappa \cdot u = f, & \forall (x, \omega) \in (0, l) \times \Omega; \\ u(0, \omega) = u(l, \omega) = 0; \\ \frac{d^2 u}{dx^2} \Big|_{(0, \omega)} = \frac{d^2 u}{dx^2} \Big|_{(l, \omega)} = 0, & \forall \omega \in \Omega; \end{cases} \quad (1)$$

where EI and κ are the beam and foundation stiffness coefficients. Both stiffness coefficients are assumed uncertain in this paper. For the consideration of existence and uniqueness of the response, the following hypotheses are required:

$$H_1 : \begin{cases} \exists \underline{\alpha}, \bar{\alpha} \in \mathbb{R}^{2+} \setminus \{0\}, \lambda([\underline{\alpha}, \bar{\alpha}]) < +\infty \text{ such that,} \\ P(\{\omega \in \Omega : EI(x, \omega) \in [\underline{\alpha}, \bar{\alpha}], \forall x \in [0, l]\}) = 1; \\ \exists \underline{\beta}, \bar{\beta} \in \mathbb{R}^{2+} \setminus \{0\}, \lambda([\underline{\beta}, \bar{\beta}]) < +\infty \text{ such that,} \\ P(\{\omega \in \Omega : \kappa(x, \omega) \in [\underline{\beta}, \bar{\beta}], \forall x \in [0, l]\}) = 1; \end{cases} \quad (2)$$

$$H_2 : f \in L^2(\Omega, \mathcal{F}, P; L^2(0, l)).$$

where $\lambda(\cdot)$ is a Borel measure: $\lambda([a, b]) = b - a$, following Bartle (1995). Hypothesis H1 ensures that the beam and foundation stiffness coefficients are positive-defined and uniformly limited in probability. Hypothesis H2 ensures that the stochastic load process has finite variance. Both hypotheses are necessary in order to employ the Lax-Milgram lemma and guarantee existence and uniqueness of the solution, as will be seen in the sequence.

2.1 Existence and uniqueness of the solution

In this section, a sketch of the proof of existence and uniqueness of the solution to the stochastic beam bending problem with random elastic properties is presented.

For fourth order stochastic operators, no such proof of existence and uniqueness of the solution has not been found in the literature.

In order to study existence and uniqueness of the solution, the variational problem associated to the strong form (Eq. 1) needs to be defined. This variational problem is defined in $V = L^2(\Omega, \mathcal{F}, P; Q)$, where:

$$Q = \left\{ u : (0, l) \times \{\omega\} \rightarrow \mathbf{R} \mid u(\cdot, \omega), \frac{d^2u}{dx^2}(\cdot, \omega) \in L^2(0, l), \right. \\ \left. u(0, \omega) = u(l, \omega) = 0 \wedge \frac{d^2u}{dx^2} \Big|_{(0, \omega)} = \frac{d^2u}{dx^2} \Big|_{(l, \omega)} = 0 \right\}, \tag{3}$$

and

$$V = \left\{ u : (0, l) \times \Omega \rightarrow \mathbf{R} \mid u \text{ is measurable} \right. \\ \left. \text{and } \int_{\Omega} \int_0^l \left[u^2 + \left(\frac{du}{dx} \right)^2 + \left(\frac{d^2u}{dx^2} \right)^2 \right] dx dP(\omega) < \infty \right\}. \tag{4}$$

Expression (4) means that, for fixed $\omega \in \Omega$, $u(\cdot, \omega) \in Q$. Similarly, for $x \in (0, l)$ fixed, $u(x, \cdot) \in L^2(\Omega, \mathcal{F}, P)$. Defining the tensorial product between $v \in L^2(\Omega, \mathcal{F}, P)$ and $w \in Q$ as $u = v.w$ (Treves, 1967), one should note that, for fixed $\omega \in \Omega$:

$$u(\cdot, \omega) = v(\cdot).w(\omega) \in Q,$$

whereas for fixed $x \in (0, l)$,

$$u(x, \cdot) = v(x).w(\cdot) \in L^2(\Omega, \mathcal{F}, P).$$

Hence, one has

$$\left. \begin{aligned} V &= L^2(\Omega, \mathcal{F}, P; Q); \\ L^2(\Omega, \mathcal{F}, P; Q) &\simeq L^2(\Omega, \mathcal{F}, P) \otimes Q; \end{aligned} \right\} \Rightarrow V \simeq L^2(\Omega, \mathcal{F}, P) \otimes Q.$$

It is also necessary to redefine the differential operator for the space obtained via tensorial product. The operator $D_x^\eta : V \rightarrow L^2(\Omega, \mathcal{F}, P) \otimes L^2(0, l)$ acts over an element $u \in V$ the following way (Matthies and Keese, 2005):

$$D_x^\eta u : \left(\frac{d^\eta v}{dx^\eta} \right) (x).w(\omega), \tag{5}$$

where $\eta \in \mathbf{N}$ and V is a Hilbert space, with internal product defined as

$$(u, v)_V = \int_{\Omega} \int_0^l (u.v + D_x^2 u.D_x^2 v)(x, \omega) dx dP(\omega). \tag{6}$$

The bilinear form $a : V \times V \rightarrow \mathbf{R}$ is defined as,

$$a(u, v) = \int_{\Omega} \int_0^l (\kappa \cdot u \cdot v + EI \cdot D_x^2 u \cdot D_x^2 v)(x, \omega) dx dP(\omega). \tag{7}$$

Finally, the variational problem associated to the strong form (Eq. 1) is defined as:

$$\begin{cases} \text{Find } u \in V \text{ such that} \\ a(u, v) = \ell(v), \forall v \in V. \end{cases} \tag{8}$$

In Eq. 8, $\ell : V \rightarrow \mathbf{R}$ is a linear functional, defined as:

$$\ell(v) = \int_{\Omega} \int_0^l (f \cdot v)(x, \omega) dx dP(\omega). \tag{9}$$

From the hypotheses of limited probability, one can show that the bi-linear form has the following properties:

Continuity:

$$\begin{aligned} |a(u, v)| &\leq \int_{\Omega} \int_0^l |\bar{\alpha} \cdot u \cdot v + \bar{\beta} \cdot D_x^2 u \cdot D_x^2 v| dx dP \\ &\leq C \left\{ \int_{\Omega} \left[\int_0^l |u|^2 dx \right]^{1/2} \left[\int_0^l |v|^2 dx \right]^{1/2} dP \right. \\ &\quad \left. + \int_{\Omega} \left[\int_0^l |D_x^2 u|^2 dx \right]^{1/2} \left[\int_0^l |D_x^2 v|^2 dx \right]^{1/2} dP \right\} \\ &\leq C \|u\|_V \|v\|_V, \end{aligned} \tag{10}$$

where $C = \max \{ \bar{\alpha}, \bar{\beta} \}$.

Coercivity:

$$\begin{aligned} a(u, u) &\geq \int_{\Omega} \int_0^l (\underline{\alpha} \cdot u^2 + \underline{\beta} \cdot D_x^2 u \cdot D_x^2 u) dx dP \\ &\geq c \int_{\Omega} \int_0^l (u^2 + D_x^2 u \cdot D_x^2 u) dx dP \\ &= c \cdot \|u\|_V^2, \end{aligned} \tag{11}$$

where $c = \min \{ \underline{\alpha}, \underline{\beta} \}$.

From the continuity and coercivity of the bilinear form, in light of the Lax-Milgram lemma, one is ensured that the variational problem defined in Eq. 6 has unique solution, and continuous dependency on the data (Babuska et al., 2005; Brenner and Scott, 1994).

3 Uncertainty representation

In most engineering problems, complete statistical information about uncertainties is not available. Sometimes, the first and second moments are the only information available. The probability distribution function is defined based on experience or heuristically. In this paper, the uncertainties on beam bending and foundation stiffness are modeled by parameterized stochastic processes, obtained from a linear combination of deterministic functions and random variables (Grigoriu, 1995),

$$\kappa(x, \omega) = \sum_{i=1}^N \phi_i(x) \xi_i(\omega), \quad (12)$$

where $\phi_i \in C_0(0, l) \cap C^1(0, l)$, $\forall i \in \{1, \dots, N\}$ are deterministic functions and $\{\xi_i\}_{i=1}^N$ are random variables. To obtain approximate solutions via the Galerkin method, a formal mathematical representation of the uncertainty is necessary. The Askey-Wiener scheme is used to represent uncertainty and to construct the solution space to the beam bending problem on Winkler foundation.

3.1 The Askey-Wiener scheme

The Askey-Wiener scheme is a generalization of chaos polynomials, also known as Wiener-chaos. Chaos polynomials were proposed by Wiener (1938) to study statistical mechanics of gases. Xiu et al. (2002) extended the ideas of Ghanem and Spanos (1991) and Ogura (1972) for polynomials belonging to the Askey-Wiener scheme (Askey and Wilson, 1985), for the representation of stochastic processes by orthogonal polynomials. The Cameron-Martin theorem (1947) shows that Askey-Wiener polynomials form a base for a dense subspace of second order random variables $L^2(\Omega, \mathcal{F}, P)$.

Let $\mathcal{H} \subseteq L^2(\Omega, \mathcal{F}, P)$ be a separable Gaussian Hilbert space and $\mathcal{H} = \text{span} [\{\xi_i\}_{i=1}^{\infty}]$ be an ortho-normal basis of Gaussian random variables. Let $P_n(\mathcal{H})$ be the vector space spanned by all polynomials of order less than n :

$$P_n(\mathcal{H}) = \left\{ \Gamma \left(\{\xi_i\}_{i=1}^N \right) : \Gamma \text{ is the polynomial of degree } \leq n; \xi_i \in \mathcal{H}, \forall i = 1, \dots, N; N < \infty \right\}, \quad (13)$$

with

$$\mathcal{H}^{:0:} = \overline{P_0}(\mathcal{H}), \mathcal{H}^{:n:} = \overline{P_n}(\mathcal{H}) \cap \overline{P_{n-1}}(\mathcal{H})^\perp, \tag{14}$$

where $\overline{P_n}$ is the closure of P_n in $L^2(\Omega, \mathcal{F}, P)$. Following Jason (1997), the space $L^2(\Omega, \Sigma(\mathcal{H}), P)$ admits the following orthogonal decomposition:

$$L^2(\Omega, \Sigma(\mathcal{H}), P) = \bigoplus_{n=0}^\infty \mathcal{H}^{:n:}, \tag{15}$$

where $\Sigma(\mathcal{H})$ is a σ - \dot{O} -algebra generated by \mathcal{H} . Hence, any second order random variable $u \in L^2(\Omega, \Sigma(\mathcal{H}), P)$ can be represented by a series expansion:

$$u(\omega) = \sum_{\iota \in \mathcal{I}} u_\iota \psi_\iota(\xi(\omega)), \tag{16}$$

where ι is a multi-index, \mathcal{I} is a set of natural numbers with compact support, $\{\psi_\iota\}_{\iota \in \mathcal{I}}$ are chaos polynomials and $\{u_\iota\}_{\iota \in \mathcal{I}}$ are coefficients of a linear combination. In Eq. 16, polynomials ψ_ι are multi-dimensional Hermite polynomials:

$$\psi_\iota(\xi(\omega)) = \prod_{m=1}^\infty h_{\iota_m}(\xi_m(\omega)), \tag{17}$$

where $h_{\iota_m}(\cdot)$ is a Hermite polynomial defined in terms of random variable ξ_m . The inner product between polynomials ψ_i and ψ_j in $L^2(\Omega, F, P)$ is defined as

$$(\psi_i, \psi_j)_{L^2(\Omega, \mathcal{F}, P)} = \int_\Omega (\psi_i \cdot \psi_j)(\xi(\omega)) dP(\omega), \tag{18}$$

where dP is a probability measure. These polynomials form a total orthonormal set (Kreyszig, 1989), with respect to the probability measure, with the following properties:

$$\psi_0 = 1, \quad (\psi_i, \psi_j)_{L^2(\Omega, \mathcal{F}, P)} = \delta_{ij}, \quad \forall i, j \in \mathbb{N}. \tag{19}$$

It is important to observe that in Eq. 19 the polynomials are orthogonal with respect to the standard Gaussian density function of vector ξ .

The Askey-Wiener scheme represents a family of sub-spaces generated by orthogonal polynomials obtained from ordinary differential equations (Xiu and Karniadakis, 2002). Among them, the Hermite, Laguerre, Jacobi and Legendre polynomials can be cited. These polynomials form a complete orthonormal set in $L^2(\Omega, \Sigma(\mathcal{H}), P)$.

The orthogonality between the polynomials is defined with respect to a weight function, which is identical to the probability density function of a certain random variable. For example, the Gaussian density function is used as weight function to obtain the orthogonality between Hermite polynomials. Table 1 shows the correspondence between subsets of polynomials of the Askey-Wiener scheme and the corresponding probability density functions.

The proposal of the Askey-Wiener scheme is to extend the result presented in Eq. 16 to other types of polynomials. In analogy to Eq. 13, taking $P_n(H) = \text{span} \left[\{\psi_i\}_{i=1}^N \right]$, with H a separable Hilbert space of finite variance random variables, one has that $\mathcal{P} = \bigcup_{n \in \mathbb{N}} P_n(H)$ is a family of polynomials of the Askey-Wiener scheme, also a complete orthonormal set in $L^2(\Omega, \mathcal{F}, P)$.

Table 1: Correspondence between some random variables and polynomials of the Askey-Wiener scheme.

Random variable	Polynomial	Weight function	Support
Gaussian	Hermite	$e^{-\frac{ \xi ^2}{2}}$	$(-\infty, +\infty)$
Gamma	Laguerre	$\frac{1}{\Gamma(v+1)} \xi^v e^{-\xi}$	$[0, +\infty)$
Beta	Jacobi	$\frac{2^{-(v+\gamma+1)} \Gamma(v+\gamma+2)}{\Gamma(v+1)\Gamma(\gamma+1)} (1-\xi)^v (1+\xi)^\gamma e^{-\xi}$	$[a, b]$
Uniform	Legendre	$\frac{1}{b-a}$	$[a, b]$

4 Galerkin Method

The Galerkin method is used in this paper to solve the stochastic beam bending problem on Winkler foundation, with uncertainties in beam and foundation stiffness coefficients. It is proposed that approximated solutions to the stochastic displacement response of the beam have the following form

$$u(x, \omega) = \sum_{i=1}^{\infty} u_i v_i(x, \omega), \tag{20}$$

where $u_i \in \mathbb{R}, \forall i \in \mathbb{N}$ are coefficients and $v_i \in V$ are the test functions. Numerical solutions to the variational problem defined in Eq. 8 will be obtained. Hence, it becomes necessary to define spaces less abstract, than those defined earlier, but without compromising the existence and uniqueness of the solution. Consider two total orthonormal sets $\Phi = \text{span} [\{\varphi_i\}_{i=1}^{\infty}]$ and Ψ , sequentially dense, such that $\overline{\Phi}^Q = Q$ and $\overline{\Psi} = \Psi$. Define the tensor product between Φ and Ψ as (Treves, 1967),

$$(\varphi \otimes \psi)_i(x, \omega) = \varphi_j(x) \cdot \psi_k(\omega), \text{ with } (j, k) \in \mathbb{N}^2. \tag{21}$$

To simplify the notation, we will use $v_i = (\varphi \otimes \psi)_i$. Since approximated numerical solutions are derived in this paper, the solution space has finite dimensions. This implies truncation of the total orthonormal sets Φ and Ψ . Hence one has $\Phi_m = \text{span}[\{\varphi_i\}_{i=1}^m]$ and $\Psi_n = \text{span}[\{\psi_i\}_{i=1}^n]$, which results in $V_M = \Phi_m \otimes \Psi_n$, with $\dim(V_M)$ and $M = m.n$. In this way, $v_i = (\varphi \otimes \psi)_i$ is the i^{th} entry of the tensor product between the base elements of two spaces with finite dimensions, (Φ_m and Ψ_n). With the above definitions and results, it is proposed that numerical solutions are obtained from truncation of the series expressed in Eq. 20 at the M^{th} term,

$$u_M(x, \omega) = \sum_{i=1}^M u_i v_i(x, \omega) \tag{22}$$

Replacing Eq. 22 in Eq. 8, one arrives at the approximated variational problem

$$\left\{ \begin{array}{l} \text{Find } \{u_i\}_{i=1}^M \in \mathbb{R}^M \text{ such that} \\ \sum_{i=1}^M a(v_i, v_j) u_i = \ell(v_j), \forall v_j \in V_M. \end{array} \right. \tag{23}$$

The approximated variational problem (Eq. 23) consists in finding the coefficients of the linear combination expressed in Eq. 22. Using a vector-matrix representation, the system of linear algebraic equations defined in Eq. 23, can be written as

$$KU = F, \tag{24}$$

where $K \in \mathbb{M}_M(\mathbb{R})$ is the stiffness matrix, $U = \{u_i\}_{i=1}^M$ is the displacement vector and $F = \{f_i\}_{i=1}^M$ is the loading vector. Elements of the stiffness matrix are defined as

$$K = [k_{ij}]_{M \times M},$$

$$k_{ij} = \int_{\Omega} \int_0^l (\kappa.v_i.v_j + EI.D_x^2 v_i.D_x^2 v_j)(x, \omega) dx dP(\omega). \tag{25}$$

The loading vector is given by,

$$F = \{f_i\}_{i=1}^M, f_i = \int_{\Omega} \int_0^l (f.v_i)(x, \omega) dx dP(\omega). \tag{26}$$

In the numerical solutions, a family of Legendre polynomials is used to construct space, defined in four independent, uniform random variables ($n_{rv}=4$). Numerical

solutions are obtained for $m = 1$, $m = \dim(\Phi_m)$, and for different orders of chaos polynomials, with $1, 2, 3, 4, 5\}$. The size of the chaos polynomial basis becomes , since $n = \frac{(p+n_r)!}{p!n_r!}$. This results in numerical solutions with $M \in \{5, 15, 35, 70, 126\}$ coefficients to determinate. The sparseness of the stiffness matrix for example 1 (to be presented) is shown in Fig. 1. Remember that “ p ” is the order of chaos polynomials. The matrix in Fig. 1a has dimension 5 and 13 non-zero elements, whereas the matrix in Fig. 1b has dimension 126 and 4754 non-zero elements.

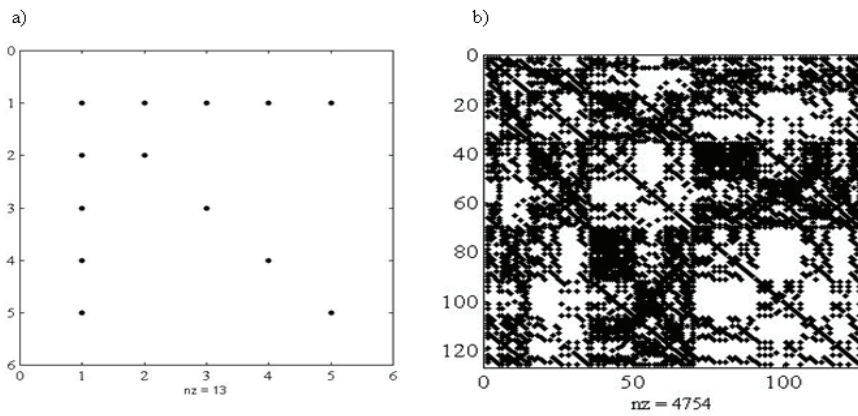


Figure 1: Sparseness of the stiffness matrix of example 1. a) for $m = 1$, $n = 5$, $p = 1$; b) for $m = 1$, $n = 126$, $p = 5$.

The conditioning numbers (nc) for these two matrixes are $nc=610.94$ and $nc=936.38$, respectively. It can be observed that the conditioning number increases with increase in dimension of the approximation space.

5 Statistical Moments

Numerical solutions to be obtained are defined in $V_M \subset L^2(\Omega, \mathcal{F}, P) \otimes Q$. From the numerical solutions for the stochastic displacement response, first and second order statistical moments are to be computed.

The statistical moment of k^{th} order of a random variable $u(x, \cdot)$ is obtained, for a fixed point $x \in [0, l]$, by taking the k^{th} power of the variable and integrating with

respect to its probability measure,

$$\begin{aligned} \mu_{u_M}^k(x) &= \int_{\Omega} u_M^k(x, \xi(\omega)) dP(\xi(\omega)) \\ &= \overbrace{\sum_{i_1} \cdots \sum_{i_k}}^{k \text{ times}} u_{i_1} \times \cdots \times u_{i_k}(\phi_{i_1} \times \cdots \times \phi_{i_k})(x) \times \\ &\quad \times \int_{\Omega} (\psi_{i_1} \times \cdots \times \psi_{i_k})(\xi(\omega)) dP(\xi(\omega)). \end{aligned} \tag{27}$$

The integration term $dP(\cdot)$ is a probability measure defined as,

$$dP(\xi(\omega)) = \prod_{i=1}^N \rho_i(\xi_i) d\xi_i(\omega), \tag{28}$$

where $\rho_i : [a_i, b_i] \rightarrow \mathbf{R}$ is the probability density function of random variable ξ_i . From the measure and integration theory (Fernandez, 2002), one knows that the measure defined in Eq. 28 is the product between probability measure spaces associated to the random variables $\xi(\omega) = \{\xi_i(\omega)\}_{i=1}^N$, with $\xi_i : \Omega \rightarrow [a_i, b_i]$. Following the uncertainty modeling assumptions made in this paper, it follows that $|[a_i, b_i]| = b_i - a_i < \infty, \forall i \in \{1, \dots, N\}$. Hence, from Eq. 27 one has,

$$\mu_{u_M}^k(x) = \overbrace{\sum_{i_1, j_1} \cdots \sum_{i_k, j_k}}^{k \text{ times}} (u_{i_1} \phi_{i_1} \times \cdots \times u_{i_k} \phi_{i_k})(x) \times \langle \psi_{i_1}, \dots, \psi_{i_k} \rangle \tag{29}$$

with

$$\begin{aligned} \langle \psi_{i_1}, \dots, \psi_{i_k} \rangle &= \int_{a_1}^{b_1} \cdots \int_{a_N}^{b_N} (\psi_{i_1} \times \cdots \times \psi_{i_k})(\xi(\omega)) \\ &\quad \times \rho_1(\xi_1) \times \cdots \times \rho_N(\xi_N) \\ &\quad \times d\xi_1(\omega) \times \cdots \times d\xi_N(\omega). \end{aligned} \tag{30}$$

The integrals in Eq. 30 are called iterated integrals. The first order statistical moment, or expected value, of the stochastic displacement process evaluated at a point $x \in [0, l]$ is

$$\mu_{u_M}(x) = \sum_{i=1}^m u_{(i-1).n+1} \phi_i(x). \tag{31}$$

The variance of the stochastic displacement process is

$$\sigma_{u_M}^2(x) = \sum_{i=1}^n \sum_{j=1}^n \sum_{k=2}^m u_{ik} u_{jk} (\varphi_i \cdot \varphi_j)(x). \tag{32}$$

In the numerical examples to follow, the statistical moments defined in Eqs. (31) and (32) are evaluated and compared with the same moments estimated via Monte Carlo simulation.

6 Numerical Examples

In this section, two numerical examples of the stochastic Euler-Bernoulli beam bending problem on Winkler foundation are presented. In both examples, the beam is simply supported at both ends, has a span of one meter, ($l = 1\text{ m}$), and rectangular cross-section with $b = \frac{1}{100}\text{ m}$ and $h = \frac{1}{50}\text{ m}$. The load term is deterministic in both cases and equal to $f(x) = 1\text{ KPa}/\text{m}$, $\forall x \in (0, 1)$. Stiffness coefficients of the beam and of the foundation have mean values of $\mu_{EI}(x) = 1400\text{ N}\cdot\text{m}^2$, $\forall x \in (0, 1)$ and $\mu_{\kappa}(x) = 1\text{ KPa}\cdot\text{m}$, $\forall x \in (0, 1)$, respectively. A graphical representation of the beam bending problem, addressed in the numerical examples, is presented in Fig. 2.

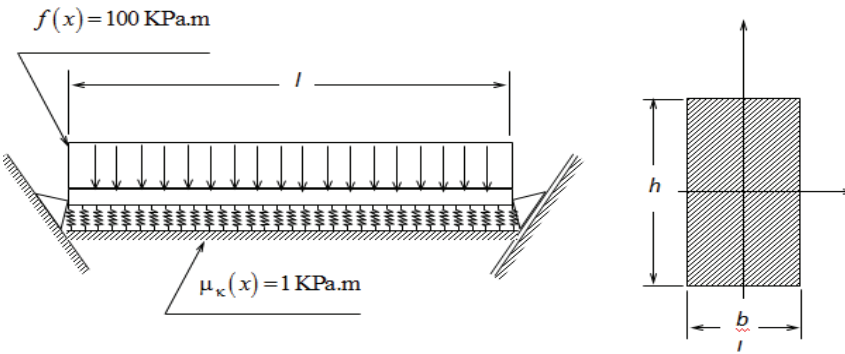


Figure 2: a) Simply supported beam subjected to uniform distributed load; b) Beam cross-section.

Expected value and variance of the numerical solutions obtained via Galerkin method are compared with the respective estimates obtained via Monte Carlo simulation. To evaluate the error of the approximated solutions, relative error functions in ex-

pected value and in variance (ε_{μ_u} and $\varepsilon_{\sigma_u^2}$, respectively), are defined as

$$\begin{aligned} \varepsilon_{\mu_u}(x) &= \begin{cases} (100\%) \times \left| 1 - \left(\frac{\mu_{uM}}{\hat{\mu}_u} \right) (x) \right|, & \forall x \in (0, 1) \\ 0, & \forall x \in \{0, 1\}; \end{cases} \\ \varepsilon_{\sigma_u^2}(x) &= \begin{cases} (100\%) \times \left| 1 - \left(\frac{\sigma_{uM}}{\hat{\sigma}_u} \right)^2 (x) \right|, & \forall x \in (0, 1) \\ 0, & \forall x \in \{0, 1\}; \end{cases} \end{aligned} \quad (33)$$

where μ_u and σ_u^2 , are the Galerkin-based expected value and variance, respectively, and $\hat{\mu}_u$ and $\hat{\sigma}_u^2$ are the Monte Carlo estimates of the same moments. Numerical results presented in this paper were obtained in a personal computer, HP-Pavilion zv 6000, running a MATLAB computational code.

6.1 Example 1: random beam stiffness

In this first example, uncertainty is considered only in the beam bending stiffness. The foundation stiffness is assumed deterministic and equal to the mean value (μ_κ). The uncertain beam stiffness is represented by a parameterized random process of the form,

$$EI(x, \omega) = \mu_{EI} + \sqrt{3} \cdot \sigma_{EI} \sum_{n=1}^{N_{EI}} \left[\xi_{2,n-1}(\omega) \cos\left(\frac{\pi}{n}x\right) + \xi_{2,n}(\omega) \sin\left(\frac{\pi}{n}x\right) \right], \quad (34)$$

where μ_{EI} is the mean value, σ_{EI} is the standard deviation and are orthogonal random variables with uniform distribution. In the example, $N_{EI} = 2$. The Galerkin method is used to obtain numerical solutions for two cases of beam stiffness standard deviation: (a) $\sigma_{EI} = \left(\frac{1}{10}\right) \cdot \mu_{EI}$ and (b) $\sigma_{EI} = \left(\frac{1}{5}\right) \cdot \mu_{EI}$. Figure 3 shows the covariance function of the beams stiffness for case (a), obtained from equation (34). It can be observed that the process is widely stationary. The covariance function shown in Fig. 3 is obtained in exact form from Eq. 34 and from the orthogonality property of random variables $\{\xi_n\}_{n=1}^{2 \cdot N_{EI}}$.

6.1.1 Results for case (a), $\sigma_{EI} = \left(\frac{1}{10}\right) \cdot \mu_{EI}$

Fig. 4 shows realizations of the stochastic displacement process of the beam. Fig. 4a shows all sampled realizations of beam displacement and Fig. 4b shows the (random variable) displacement at mid-span, obtained by fixing $x = \frac{1}{2}$.

Fig. 5 shows convergence of Monte Carlo simulation results, for mean value and standard deviation of $u\left(\frac{1}{2}, \cdot\right)$, as function of the number of samples N . The figure

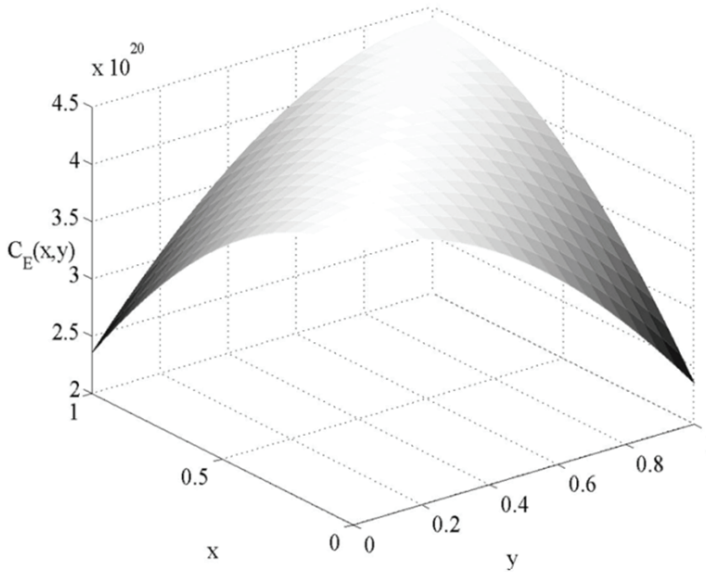


Figure 3: Covariance function of beam stiffness.

shows that convergence of simulation results is achieved for $N > 1500$, and that the number of samples considered ($N_s = 5000$) is sufficient.

Fig. 6 shows the expected value of the stochastic displacement process and the relative error, for Galerkin solutions using chaos polynomials of order $p \in \{1, 2, 3, 4, 5\}$. It is observed that, for increasing values of “ p ” the approximated solution for expected value approaches simulation results. It is important to note that some of the curves accumulate over each other (for $p \geq 3$), and no difference can be observed between them. The relative error shown in Fig. 6b is better to illustrate convergence of the expected value to the Monte Carlo estimate.

In Fig. 7 the variance of stochastic displacement process is shown. Fig. 7a shows that the variance is well represented by the approximated Galerkin solution for $p = 2$ or more. Fig. 7b shows the relative error in variance and convergence of this solution in terms of the polynomial order. The behavior is similar to that observed for the mean value.

It is important to note that, despite the stochastic beam bending stiffness being a widely stationary process, the stochastic displacement process is not; this fact can be observed in Figs. 6a and 7a. This result shows influence of the mathematical model, Eq.(1), in the propagation of uncertainty from system properties to the

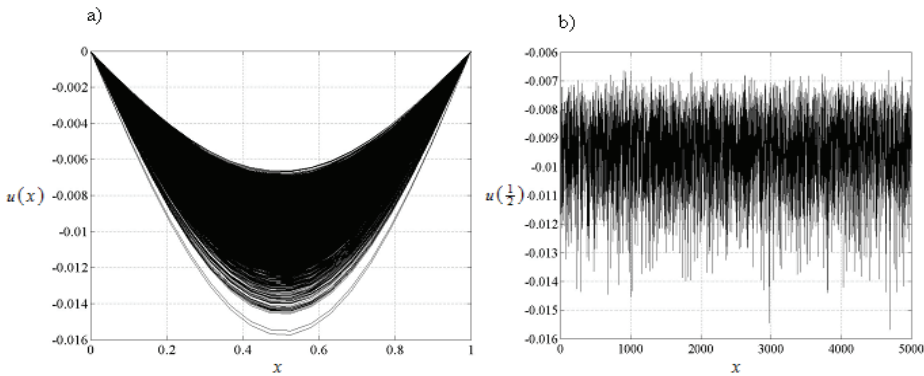


Figure 4: a) Realizations of the stochastic displacement process; b) random variable $u(\frac{1}{2})$.

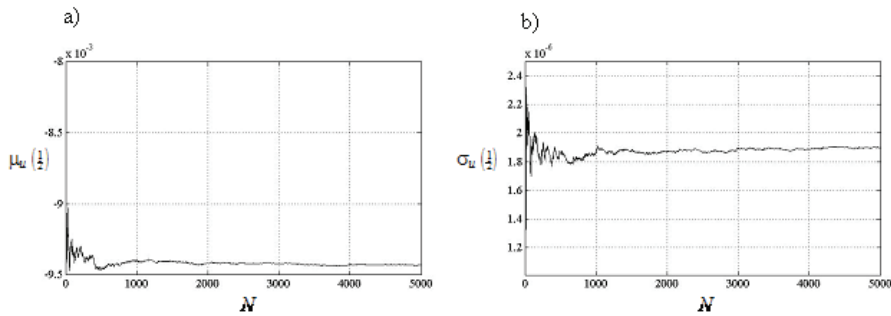


Figure 5: a) Convergence in expected value for $u(\frac{1}{2}, \cdot)$; b) Convergence in standard deviation for $u(\frac{1}{2}, \cdot)$.

solution. In this case, the stationarity is not preserved.

6.1.2 Results for case (b), $\sigma_{EI} = (\frac{1}{5}) \cdot \mu_{EI}$

Fig. 8 shows convergence of Monte Carlo simulation results as function of number of samples N , in terms of mean value and standard deviation of $u(\frac{1}{2}, \cdot)$, for case (b). This figure shows convergence of the Monte Carlo statistics for $N > 4000$. Comparing Figs. 5a and 8a, one notes that the expected value of mid-span displacement for case (b) is larger than for case (a). The variance (Figs. 5b and 8b) for case (b) is also larger.

Fig. 9 shows the expected value of the stochastic displacement process (Fig. 9a)

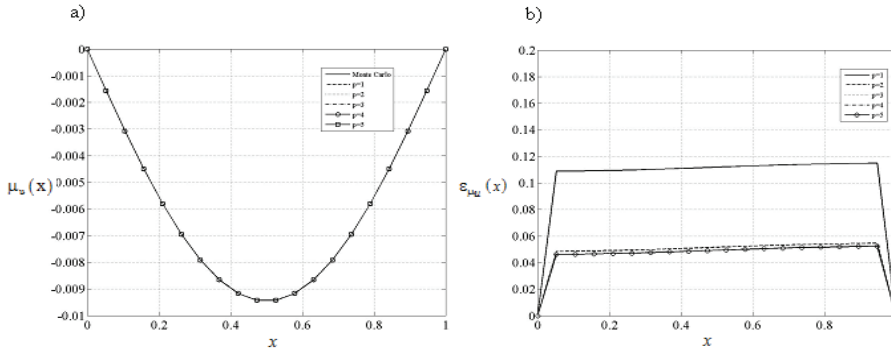


Figure 6: a) Expected value of the stochastic displacement process; b) Relative error in expected value.

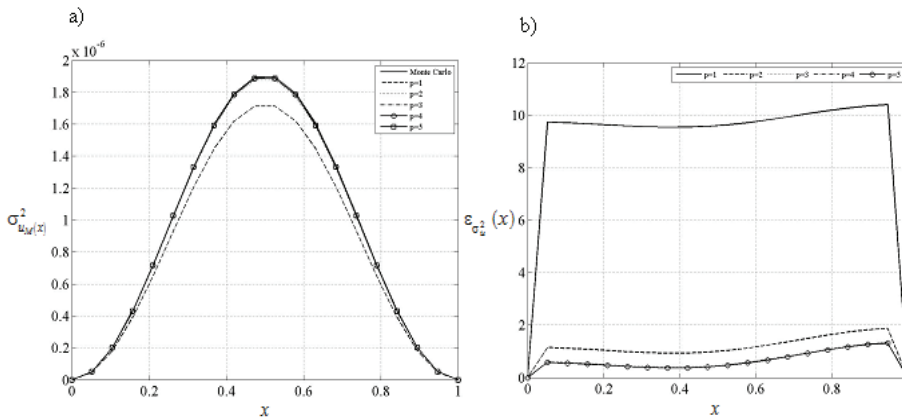


Figure 7: a) Variance of the stochastic displacement process; b) Relative error in variance.

and the relative error (Fig. 9b), for Galerkin solutions using chaos polynomials of order $p \in \{1, 2, 3, 4, 5\}$. It is observed that, for increasing values of “ p ”, the approximated expected value converges to the simulation result. Fig. 9b shows that the relative error in expected value is reduced as the order of approximated solution polynomials is increased. This behavior is similar to what was observed for case (a).

Fig. 10 shows variance of the stochastic displacement process. Fig. 10a shows that the variance, obtained from the approximated solution, accumulates over the corresponding Monte Carlo statistic for $p = 4$. Comparing Fig 7b and 10b, similar

behavior is observed for the relative error in variance, for both cases.

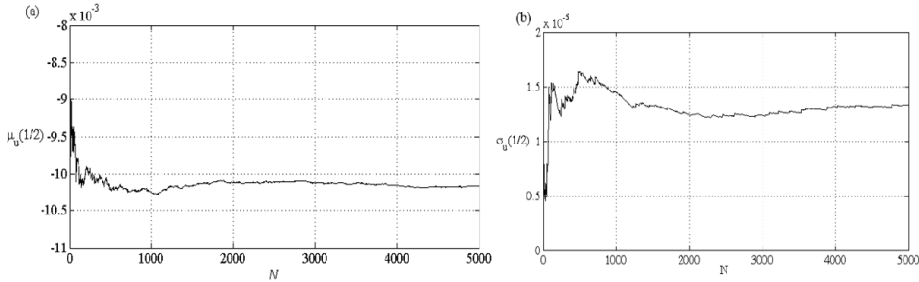


Figure 8: a) Convergence in expected value for $u\left(\frac{1}{2}, \cdot\right)$; b) Convergence in standard deviation for $u\left(\frac{1}{2}, \cdot\right)$.

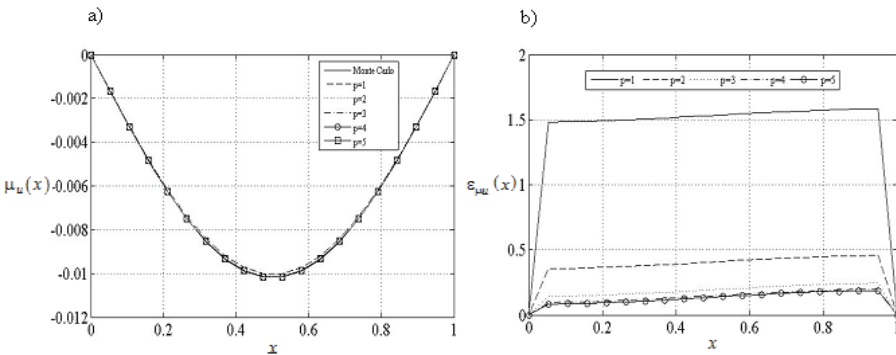


Figure 9: a) Expected value of stochastic displacement process; b) Relative error in expected value.

6.1.3 Summary of results for cases (a) and (b)

Tab. 2 summarizes results of expected value, variance and corresponding relative errors for the random variable obtained by fixing $x = \frac{1}{2} m$ in the stochastic displacement process, for cases (a) and (b) of example 1. Results are presented for approximated solutions with $p \in \{1, 2, 3, 4, 5\}$. Monte Carlo estimates of expected value and variance for cases (a) and (b) were obtained as:

$$\hat{\mu}_u\left(\frac{1}{2}\right) = -0.00942931964845653 \text{ m};$$

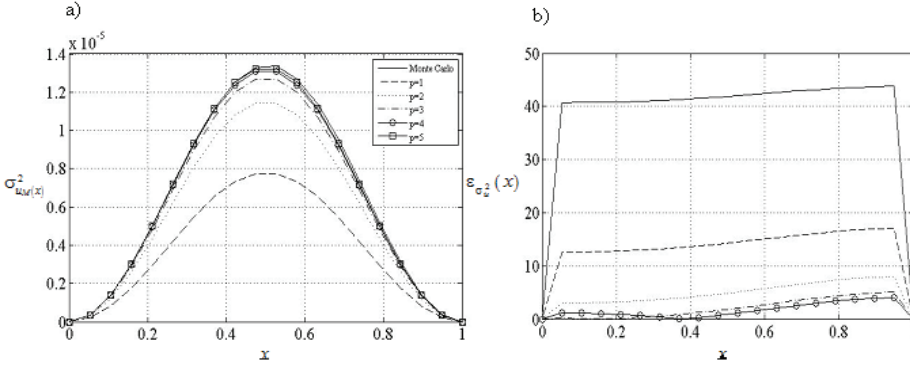


Figure 10: a) Variance of stochastic displacement process; b) Relative error in variance.

$$\hat{\sigma}_u^2\left(\frac{1}{2}\right) = 1.89469499239802 \times 10^{-6} \text{m}^2;$$

and

$$\hat{\mu}_u\left(\frac{1}{2}\right) = -0.0101664271222058 \text{ m};$$

$$\hat{\sigma}_u^2\left(\frac{1}{2}\right) = 1.32950337865645 \times 10^{-5} \text{m}^2.$$

Comparing Monte Carlo estimates for expected value and variance with results obtained via approximated Galerkin solutions, one notes that approximated results are smaller in both cases. Table 2 also shows that, for case (a), the expected value and variance of random variable $u\left(\frac{1}{2}, \cdot\right)$ is smaller than for case (b). The same behavior is observed for the Monte Carlo estimates of expected value and variance, for this random variable.

In this example, it is observed that the statistical moments are well represented by the approximated solution, for chaos polynomials of order $p = 3$. The relative error function for variance, in both cases and for $x = \frac{1}{2} m$, decreases sharply as the order of polynomial chaos increases.

Table 2: Summary of numerical results for cases (a) and (b) of example 1: expected value, variance, relative errors in expected value and variance for the stochastic displacement process at mid-span ($x = \frac{1}{2}$).

$p(M)$	case (a)			
	$\mu_{UM}(\frac{1}{2})$	$\sigma_{UM}^2(\frac{1}{2})$	$\epsilon_{\mu}(\frac{1}{2})$	$\epsilon_{\sigma^2}(\frac{1}{2})$
1 (5)	-0.00941874489365295	$1.71325528999495 \times 10^{-6}$	0.1149165598530700	10.4025644709826
2 (15)	-0.00942443119453395	$1.87624312769187 \times 10^{-6}$	0.0546137653324747	1.87885386851441
3 (35)	-0.00942464045330815	$1.88638407354279 \times 10^{-6}$	0.0523945917209326	1.34851682686812
4 (70)	-0.00942464883037076	$1.88695783644589 \times 10^{-6}$	0.0523057536000271	1.31851097483937
5 (126)	-0.00942464918385567	$1.88698917798115 \times 10^{-6}$	0.0523020049188037	1.31687191894457
$p(M)$	case (b)			
	$\mu_{UM}(\frac{1}{2})$	$\sigma_{UM}^2(\frac{1}{2})$	$\epsilon_{\mu}(\frac{1}{2})$	$\epsilon_{\sigma^2}(\frac{1}{2})$
1 (5)	-0.0100101240864717	$7.74060536291528 \times 10^{-6}$	1.583857884720170	43.7970549261655
2 (15)	-0.0101246383965768	$1.14205613180607 \times 10^{-5}$	0.457992059264072	17.077650858584
3 (35)	-0.0101463112185796	$1.26714743829824 \times 10^{-5}$	0.244912230098401	7.99502811973357
4 (70)	-0.0101510485401449	$1.30776138143105 \times 10^{-5}$	0.198336492536587	5.04613315854419
5 (126)	-0.0101521882209810	$1.32094708185086 \times 10^{-5}$	0.187131537416978	4.08874654379080

6.2 Example 2: random foundation stiffness

In this example, uncertainty in the foundation stiffness coefficient is considered. This uncertainty is modeled by a parameterized stochastic process:

$$\kappa(x, \omega) = \mu_\kappa + \sqrt{3} \cdot \sigma_\kappa \sum_{n=1}^{N_\kappa} [\xi_{2,n-1}(\omega) \cos\left(\frac{\pi}{n}x\right) + \xi_{2,n}(\omega) \sin\left(\frac{\pi}{n}x\right)], \quad (35)$$

where μ_κ is the mean value, σ_κ is the standard deviation and $\{\xi_{2,n}\}$ are independent random variables with uniform distribution. In this example, $N_\kappa = 2$ is used. Numerical solutions are obtained for two cases of standard deviation: (a) $\sigma_\kappa = \left(\frac{1}{10}\right) \cdot \mu_\kappa$ and (b) $\sigma_\kappa = \left(\frac{1}{5}\right) \cdot \mu_\kappa$. As in example 1, the random foundation stiffness coefficient is widely stationary.

6.2.1 Results for case (a), $\sigma_\kappa = \left(\frac{1}{10}\right) \cdot \mu_\kappa$

Fig. 11 shows realizations of the stochastic displacement process of the beam. Fig. 11a shows all sampled realizations of beam displacement and Fig. 11b shows the (random variable) displacement at mid-span, obtained by fixing $x = \frac{1}{2}$.

Fig. 12 shows convergence of Monte Carlo simulation results as function of number of samples N , in terms of mean value and standard deviation of $u\left(\frac{1}{2}, \cdot\right)$. Convergence of Monte Carlo estimates can be observed for $N > 2000$.

Figure 13 shows convergence of Galerkin results in terms of expected value (Fig. 13a) and relative error (Fig. 13b) for polynomial chaos of order $p \in \{1, 2, 3, 4, 5\}$. It is observed that, for $p = 1$ or greater, the expected value functions accumulate over each other, and the curves are indistinguishable.

Comparing Fig 6b and 13b, one notes that the relative error in expected value is larger for case (a) of example 1, in comparison to case (a) of example 2.

Figure 14 shows the variance and the relative error function for variance of stochastic displacement process. Comparing Figs. 7a and 14a it is observed that the dispersion, measured in terms of variance, is smaller for this example than it was observed for example 1, case (a).

6.2.2 Results for case (b), $\sigma_\kappa = \left(\frac{1}{5}\right) \cdot \mu_\kappa$

Figure 15 shows convergence of Monte Carlo simulation results as function of number of samples N , in terms of mean value and standard deviation of $u\left(\frac{1}{2}, \cdot\right)$, for case (b). Comparing Figs. 12a and 15a, it can be observed that the mean values for case (b) and (a) are close. The standard deviation, however, is larger for case (b). The figure shows convergence of Monte Carlo statistics for $N > 1500$.

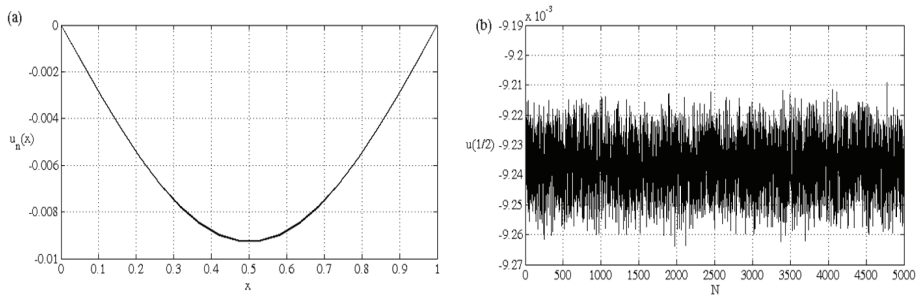


Figure 11: a) Realizations of the stochastic displacement process; b) random variable.

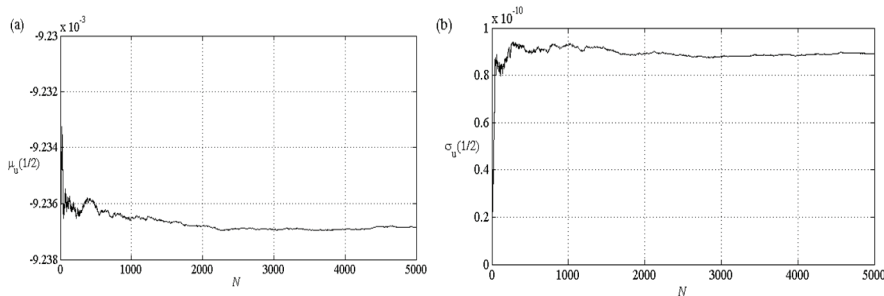


Figure 12: a) Convergence in expected value for $u\left(\frac{1}{2}, \cdot\right)$; b) Convergence in standard deviation for $u\left(\frac{1}{2}, \cdot\right)$.

Figure 16 shows the expected value of random displacement response obtained via Galerkin method, and the relative error of this result. Fig. 16a shows that, for different values of “ p ”, the expected value of beam displacement accumulates over the Monte Carlo estimate. Fig. 16b emphasizes this result, by showing the relative error in expected value for $p \in \{1, 2, 3, 4, 5\}$.

Fig. 17 shows variance of the stochastic displacement process and the corresponding relative error. It can be observed that the dispersion, in terms of variance, is larger for the approximated solutions in comparison to the variance obtained via simulation. The behavior observed in Fig. 17b is similar to Fig. 16b, where the results for relative error in variance accumulate over each other for different values of “ p ”. It is also observed that the relative error in expected value is smaller than the relative error in variance.

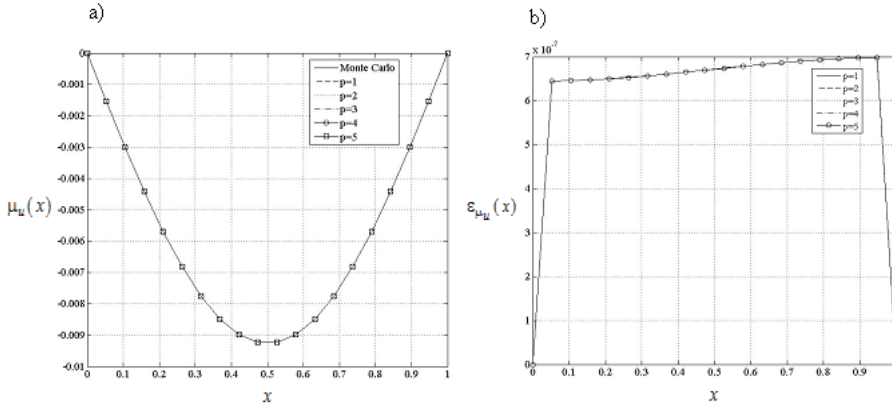


Figure 13: a) Expected value of the stochastic displacement process; b) Relative error in expected value.

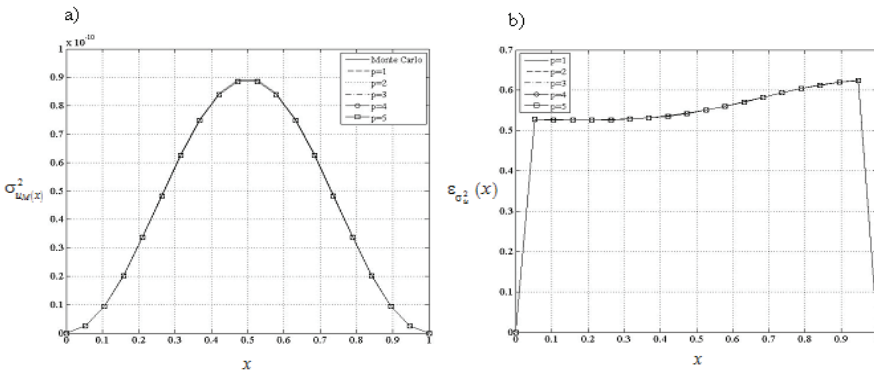


Figure 14: a) Variance of stochastic displacement process; b) Relative error in variance.

6.3 Summary of results for cases (a) and (b)

Results of expected value, variance and corresponding relative errors for the random variable obtained by fixing $x = \frac{1}{2}$ in the stochastic displacement process, for cases (a) and (b) of example 2, are summarized in Table 3. Results are presented for approximated solutions with $p \in \{1, 2, 3, 4, 5\}$. Monte Carlo estimates of expected value and variance for cases (a) and (b) were obtained as:

$$\hat{\mu}_u\left(\frac{1}{2}\right) = -0.00923685607734612 \text{ m};$$

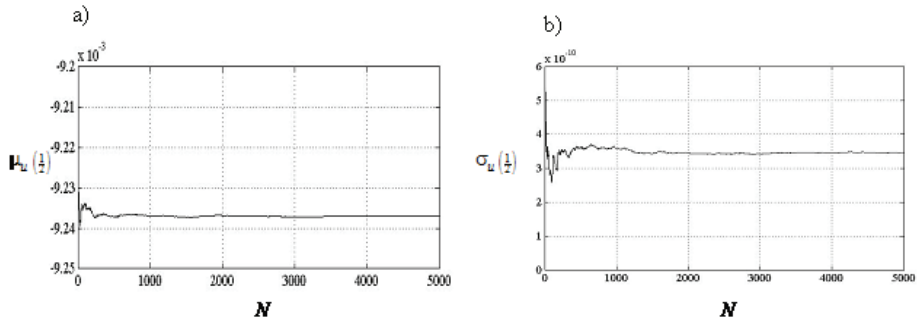


Figure 15: a) Convergence in expected value for $u\left(\frac{1}{2}, \cdot\right)$; b) Convergence in standard deviation for $u\left(\frac{1}{2}, \cdot\right)$.

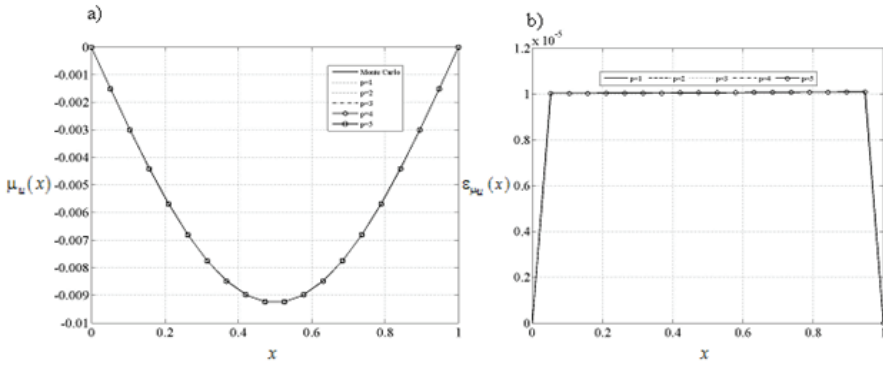


Figure 16: a) Expected value of the stochastic displacement process; b) Relative error in expected value.

$$\hat{\sigma}_u^2\left(\frac{1}{2}\right) = 8.908274494156 \times 10^{-11} \text{m}^2;$$

and

$$\hat{\mu}_u\left(\frac{1}{2}\right) = -0.00923688386180743 \text{ m};$$

$$\hat{\sigma}_u^2\left(\frac{1}{2}\right) = 3.45434414766091 \times 10^{-10} \text{m}^2.$$

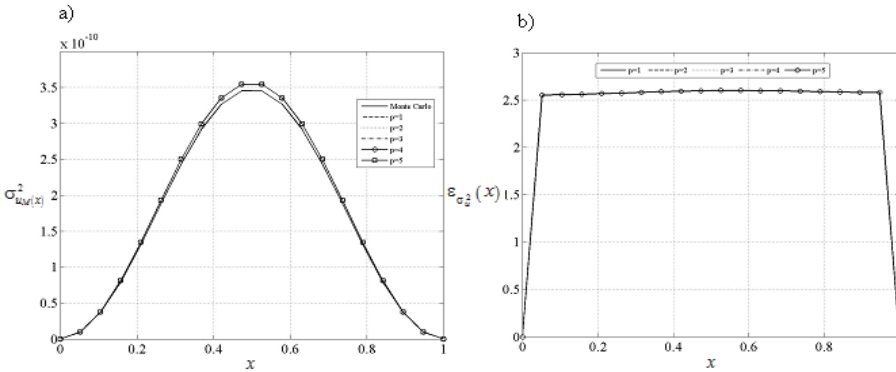


Figure 17: a) Variance of the stochastic displacement process; b) Relative error in variance.

In Table 3 it can be observed that the expected value of random variable $u(\frac{1}{2}, \cdot)$ increases as the variance of the foundation stiffness coefficient increases. For both examples, the expected value obtained from the approximated solutions at $x = \frac{1}{2}$ is slightly larger than the estimate of the same moment obtained via simulation. It is observed that, for $p = 3$ or greater, the relative error functions in expected value and variance, evaluated at $x = \frac{1}{2}$, do not change. For $p = 2$ it is observed that error functions evaluated at $x = \frac{1}{2}$ are smaller than the error for other values of “ p ”. This shows that for $p = 2$ the moments evaluated via Galerkin method at $x = \frac{1}{2}$ provided the best approximation to Monte Carlo results. The variance evaluated at $x = \frac{1}{2}$ for problem 2a is smaller than its Monte Carlo estimate, whereas for problem 2b this variance is larger than the simulation estimate. In example 2b, the best estimates for expected value and variance of transverse displacements, at $x = \frac{1}{2}$, is obtained for $p = 1$. In distinction to what was observed for example 1, in example 2 it is observed that the relative error functions in expected value and variance increase, as the polynomial order is increased above $p = 1$.

6.3.1 Summary of processing time results for examples 1 and 2, cases (a) and (b)

Table 4 summarizes results of CPU processing time for the approximated Galerkin and Monte Carlo simulation solutions of examples 1 and 2, cases (a) and (b). In interpreting these results, it is important to note that Galerkin solutions were obtained using symbolic integration in MATLAB. Use of numerical integration would likely speed up the Galerkin solutions, especially for high polynomial orders.

Results obtained herein show that the rate of convergence is larger for example 1a

Table 3: Summary of numerical results for cases (a) and (b) of example 2: expected value, variance, relative errors in expected value and variance for the stochastic displacement process at mid-span ($x = \frac{1}{2}$).

$p(M)$	case (a)			
	$\mu_{u_M}(\frac{1}{2})$	$\sigma_{u_M}^2(\frac{1}{2})$	$\epsilon_{\mu_u}(\frac{1}{2})$	$\epsilon_{\sigma_u^2}(\frac{1}{2})$
1 (5)	-0.00923685601508401	$8.85990994998009 \times 10^{-11}$	$6.74061695255010 \times 10^{-7}$	0.551042972236728
2 (15)	-0.00923685602733075	$8.85997186668474 \times 10^{-11}$	$5.41476086985778 \times 10^{-7}$	0.550347981911298
3 (35)	-0.00923685601509934	$8.85995242558453 \times 10^{-11}$	$6.73895732385947 \times 10^{-7}$	0.550566200510562
4 (70)	-0.00923685601509934	$8.85995241880827 \times 10^{-11}$	$6.73895732385947 \times 10^{-7}$	0.550566276571420
5 (126)	-0.00923685601509934	$8.85995242570788 \times 10^{-11}$	$6.73895732385947 \times 10^{-7}$	0.550566199126014
$p(M)$	case (b)			
	$\mu_{u_M}(\frac{1}{2})$	$\sigma_{u_M}^2(\frac{1}{2})$	$\epsilon_{\mu_u}(\frac{1}{2})$	$\epsilon_{\sigma_u^2}(\frac{1}{2})$
1 (5)	-0.00923688479093611	$3.54398606125908 \times 10^{-10}$	$1.00843580526973 \times 10^{-5}$	2.59770055843298
2 (15)	-0.00923688479118136	$3.54405402187884 \times 10^{-10}$	$1.00870131956034 \times 10^{-5}$	2.59966801463726
3 (35)	-0.00923688479118136	$3.54405402318379 \times 10^{-10}$	$1.00870132098173 \times 10^{-5}$	2.59966803647427
4 (70)	-0.00923688479118136	$3.54405402282752 \times 10^{-10}$	$1.00870132098173 \times 10^{-5}$	2.59966802293038
5 (126)	-0.00923688479118136	$3.54405402296312 \times 10^{-10}$	$1.00870132098173 \times 10^{-5}$	2.59966803845165

in comparison to example 2a. The same is observed for example 1b in comparison to example 2b. For all cases and examples studied, CPU time to obtain the approximated solutions for $p = 3$ or higher was larger than the time required to obtain the Monte Carlo simulation result. However, results show that the relative error in expected value and variance do not improve considerably for $p = 3$ or higher, hence approximated solutions with $p = 2$ are sufficiently accurate. In all examples and cases studied, the relative error in expected value resulted smaller than the relative error in variance. In all cases, the expected value and variance of beam displacement resulted larger for example 1 in comparison to example 2. The relative error functions for expected value and variance at $x = \frac{1}{2}m$ were also found to be higher for example 1 than for example 2. Hence, one concludes that propagation of the uncertainty to the solution is larger for the random beam stiffness in comparison to the random foundation stiffness.

For all cases studied, the approximated Galerkin solution for expected value was able to reproduce the observed simulation result. This shows the robustness of the Galerkin method and chaos polynomials in representing random beam responses for the different cases of elastic properties of the beam and of the foundation.

7 Conclusions

In this paper, the Galerkin method was applied in the solution of a stochastic Euler-Bernoulli beam bending problem, with uncertainty in bending and foundation stiffness coefficients. Random stiffness parameters were represented by parameterized stochastic processes. The approximated solution space was constructed by the tensor product between measure spaces of finite dimensions. Legendre polynomials, derived from the Askey-Wiener scheme, were used to construct the approximated solution space. Expected value and variance of transverse beam displacements were computed from the approximated Galerkin solutions and compared, in two numerical examples, with the same estimates obtained via Monte Carlo simulation.

In the first example, an uncertain beam bending stiffness was considered. In the second example, uncertain stiffness of the Winkler foundation was considered. The examples have shown that propagation of the uncertainty to beam response (transverse displacement) is larger when uncertainty is in the beam bending stiffness. For the uncertain foundation stiffness, convergence of the Galerkin solution in expected value and variance of beam displacement is faster, in comparison to the problem with uncertain beam stiffness. In general, it was observed that the approximated solutions converge for low orders of polynomial interpolation p . The Galerkin solution yielded very good estimates of the first and second order moments, even at very low orders. For the uncertain foundation stiffness problem, convergence was obtained for $p = 1$. For the uncertain beam stiffness problem with $\sigma_{EI} = \left(\frac{1}{10}\right) \cdot \mu_{EI}$,

Table 4: CPU processing time for approximated Galerkin and Monte Carlo simulation solutions of examples 1 and 2, cases (a) and (b).

Example (case)	CPU time [s], Monte Carlo simulation	CPU time [s], Galerkin solution				
		$p = 1$	$p = 2$	$p = 3$	$p = 4$	$p = 5$
1 (a)	53.40	22.14	160.80	886.08	1183.92	7232.98
1 (b)	59.50	14.41	105.95	578.67	2818.72	6336.17
2 (a)	92.84	10.23	115.31	257.95	1118.23	7104.78
2 (b)	94.30	4.09	25.75	156.23	1025.73	7662.98

convergence was obtained for $p = 2$. For the same problem with $\sigma_{EI} = \left(\frac{1}{5}\right) \cdot \mu_{EI}$, $p = 3$ was required for convergence. For the Galerkin solution, it was shown that CPU processing time increases drastically with the order of polynomial interpolation.

The Askey-Wiener Galerkin scheme presented herein presented fast convergence in the approximation of first and second order moments of the random beam displacements. The method is shown to be a theoretically sound and efficient method for the solution of stochastic problems in engineering.

Acknowledgement: Sponsorship of this research project by the São Paulo State Foundation for Research - FAPESP (grant number 2008/10366-4) and by the National Council for Research and Development - CNPq (grant number 305120/2006-9) is greatly acknowledged.

References

Anders, M.; Hori, M. (1999): Stochastic finite element method for elasto-plastic body. *International Journal for Numerical Methods in Engineering*, vol. 46, no. 11, pp. 1897-1916.

Araújo, J. M.; Awruch, A. M. (1994): On stochastic finite elements for structural analysis. *Computers and Structures*, vol. 52, no. 3, pp. 461-469.

Askey, R.; Wilson, J. (1985): Some Basic Hypergeometric Polynomials that Generalize Jacobi Polynomials. *Mem. Amer. Math. Soc.* 319, AMS, Providence, RI.

Babuska I.; Chatzipantelidis P. (2002): On solving elliptic stochastic partial differential equations. *Computer Methods in Applied Mechanics and Engineering*, vol. 191, pp. 4093-4122.

Babuska, I.; Tempone, R.; Zouraris, G. E. (2005): Solving elliptic boundary value problems with uncertain coefficients by the finite element method: the stochastic formulation. *Computer Methods in Applied Mechanics and Engineering*, vol. 194, no. 12-16, pp. 1251-1294.

Baker, R.; Zeitoun, D. G. (1990): Application of Adomian's decomposition procedure to the analysis of a beam on random Winkler support. *International Journal of Solids and Structures*, vol. 26, no. 2, pp. 217-235.

Bartle, R. G. (1995): *The Elements of Integration and Lebesgue Measure*. Wiley-Interscience.

Brenner, S. C.; Scott, L. R. (1994): *The Mathematical Theory of Finite Element Methods*. Springer-Verlag.

Cameron, R. H.; Martin, W. T. (1947): The orthogonal development of nonlinear functionals in series of Fourier-Hermite functionals. *Annals Mathematics*, no. 48,

pp. 385-392.

Chakraborty, S.; Sarkar S. K. (2000): Analysis of a curved beam on uncertain elastic foundation. *Finite Elements in Analysis and Design*, vol. 36, no. 1, pp. 73-82.

Elishakoff, I.; Ren, Y. J.; Shinozuka, M. (1995): Some exact solutions for the bending of beams with spatially stochastic stiffness. *International Journal of Solids and Structures*, vol. 32, no. 16, pp. 2315-2327.

Elman, H.; Furnival, D. (2007): Solving the stochastic steady state diffusion problem using multigrid *IMA Journal of Numerical Analysis*, no. 27, pp. 675-688.

Fernandez, P. J. (2002): *Medida e Integração*. IMPA (in Portuguese).

Ghanem, R.; Spanos, P.D. (1991): *Stochastic Finite Elements: A Spectral Approach*. Dover.

Grigoriu, M. (1995): *Applied Non-Gaussian Processes: Examples, Theory, Simulation, Linear Random Vibration, and Matlab Solutions*. Prentice Hall.

Hisada, T., Nakagiri, S. (1981): Stochastic finite element method developed for structural safety and reliability. *Proceedings of the 3rd International Conference on Structural Safety and Reliability*, Elsevier, Amsterdam, p.395-408.

Jason, S. (1997): *Gaussian Hilbert Spaces*. Cambridge University Press.

Kreyszig, E. O. (1989): *Introductory Functional Analysis with Applications*, Wiley.

Liu, N., Liu, T. G. (1996): Spectral stochastic finite element analysis of periodic random thermal creep stress in concrete. *Engineering Structures*, v. 18, n. 9, p. 669-674.

Matthies, H. G.; Keese A. (2005): Galerkin methods for linear and nonlinear elliptic stochastic partial differential equations. *Computer Methods in Applied Mechanics and Engineering*, vol. 194, no. 12-16, pp. 1295-1331.

Ogura, H. (1972): Orthogonal functionals of the Poisson process. *IEEE Trans. Inform. Theory*, vol. 18, no. 4, pp. 473-481.

Silva Jr., C.R.A. (2004): Application of the Galerkin method to stochastic bending of Kirchhoff plates, Doctoral Thesis, Department of Mechanical Engineering, Federal University of Santa Catarina, Florianópolis, SC, Brazil (in Portuguese).

Singh, B. N.; Kumar L. R. (2008): Nonlinear bending response of laminated composite plates on nonlinear elastic foundation with uncertain system properties. *Engineering Structures*, vol. 30, no. 4, pp. 1101-1112.

Spanos, P. D.; Ghanem, R. (1989): Stochastic finite element expansion for media random. *Journal Engineering Mechanics*, vol. 125, no. 1, pp. 2640.

Treves, F. (1967): *Topological Vector Spaces, Distributions and Kernels*. Academic Press.

Vanmarcke, E. H.; Grigoriu, M. (1983): Stochastic finite element analysis of simple beams. *Journal of Engineering Mechanics*, vol. 109, no. 5, pp. 1203–1214.

Wiener, N. (1938): The homogeneous chaos. *American Journal Mathematics*, no. 60, pp. 897–936.

Xiu, D.; Lucor, D.; Su C. H.; Karniadakis, G.E. (2002): Stochastic Modeling of Flow-Structure Interactions using Generalized Polynomial Chaos. *J. Fluids Engrg.*, no. 124, pp. 51-59.

Yamazaki, F.; Shinozuka, M.; Dasgupta, G. (1988): Neumann expansion for stochastic finite element analysis. *Journal of Engineering Mechanics, ASCE*. vol. 114, no. 8, pp. 1335–1354.

